Downloaded from rsfs.royalsocietypublishing.org on November 12, 2012

Interface Focus

On the topology of chromatin fibres

Maria Barbi, Julien Mozziconacci, Jean-Marc Victor, Hua Wong and Christophe Lavelle

Interface Focus 2012 **2**, 546-554 first published online 1 February 2012
doi: 10.1098/rsfs.2011.0101

References

This article cites 54 articles, 20 of which can be accessed free
http://rsfs.royalsocietypublishing.org/content/2/5/546.full.html#ref-list-1

Article cited in:
http://rsfs.royalsocietypublishing.org/content/2/5/546.full.html#related-urls

Subject collections

Articles on similar topics can be found in the following collections

biomathematics (26 articles)
biophysics (19 articles)

Email alerting service

Receive free email alerts when new articles cite this article - sign up in the box at the top right-hand corner of the article or click **here**

To subscribe to *Interface Focus* go to: **http://rsfs.royalsocietypublishing.org/subscriptions**

Downloaded from rsfs.royalsocietypublishing.org on November 12, 2012

Interface Focus

Interface Focus (2012) **2**, 546–554
doi:10.1098/rsfs.2011.0101
Published online 1 February 2012

On the topology of chromatin fibres

Maria Barbi[1,*], Julien Mozziconacci[1], Jean-Marc Victor[1], Hua Wong[2] and Christophe Lavelle[3]

[1]*Laboratoire de Physique Théorique des la Matière condensée, CNRS UMR 7600, Université Pierre et Marie Curie, Case Courrier 121, 4 place Jussieu 75252, Paris Cedex 05, France*
[2]*Institut Pasteur, 25–28 rue du Docteur Roux, 75015 Paris, France*
[3]*CNRS, National Museum of Natural History, 43 rue Cuvier, 75005 Paris, France*

The ability of cells to pack, use and duplicate DNA remains one of the most fascinating questions in biology. To understand DNA organization and dynamics, it is important to consider the physical and topological constraints acting on it. In the eukaryotic cell nucleus, DNA is organized by proteins acting as spools on which DNA can be wrapped. These proteins can subsequently interact and form a structure called the chromatin fibre. Using a simple geometric model, we propose a general method for computing topological properties (*twist*, *writhe* and *linking number*) of the DNA embedded in those fibres. The relevance of the method is reviewed through the analysis of magnetic tweezers single molecule experiments that revealed unexpected properties of the chromatin fibre. Possible biological implications of these results are discussed.

Keywords: chromatin; topology; DNA

1. DNA SUPERCOILING AND TRANSCRIPTION

According to the 'central dogma' of molecular biology, the DNA double helix codes for the sequence of all proteins in the cell. However, in eukaryotic cells, the coding sequences can vary from 90 per cent (in yeast) to less than 1.5 per cent of the DNA sequence (in higher eukaryotes, such as humans). A role of non-coding DNA in the assembling of the hierarchical architecture of the genome has been, therefore, proposed. This architecture must, at a time, compact DNA in the nucleus and let it be accessible when requested by the cell functioning. Besides the geometrical puzzling that these questions imply, the architecture of DNA and its dynamical modifications have to deal with the mechanical response of DNA that behaves as a rather rigid screw.

In particular, gene transcription imposes strong mechanical constraints. The crucial step of protein synthesis, the transcription elongation, is performed by a dedicated enzyme, the RNA-polymerase (RNAP). RNAP opens locally the double helix, reads it and makes a copy of the coding DNA template onto a RNA stretch. The transcription activation requires the formation of a large protein complex, consisting of up to 60 different proteins. Owing to the large dimension of the transcription complex, it is very unlikely that the RNAP rotates around DNA during the elongation process [1]: the DNA has, therefore, to rotate inside the RNAP. This process leads to topological and mechanical constraints upstream and downstream of the transcription site. Indeed, as the elongation complex progresses along the genomic sequence, the DNA double helix in front of it becomes overwound (positively supercoiled), whereas the DNA behind it becomes underwound (negatively supercoiled). This is the so-called twin-supercoiled-domain (TSD) model, first introduced by Liu & Wang [2] and extensively acknowledged since (for a review, see Lavelle [3]). In this paper, we will deal with the problem of building the appropriate theoretical frame where mechanical and topological constraints acting on DNA can be accounted for, in the perspective of studying the implications of these constraints for different biological processes.

2. DNA TOPOLOGY AND WHITE–FULLER THEOREM

Topology of DNA is a long-standing problem, since Vinograd *et al.* [4] introduced in 1965 the idea that the conformation of DNA both in eukaryotes and prokaryotes is related to topological quantities. They showed that circular DNA chromosomes isolated from small viruses may be in a highly compact and wrapped conformation. A proper characterization of the different conformations, or 'topoisomers' (as those displayed in figure 1) was then introduced soon after by Fuller with the mathematical definition of the three relevant topological quantities, namely the twist Tw, the writhe Wr and the linking number Lk [6,7].

Since then, a rather large amount of work has been done to study the relationship between twist and writhe for closed and open curves, especially in relation to torsionally stressed DNA including in the presence of binding proteins [8–12]. We largely refer to these works in the following derivations.

*Author for correspondence (barbi@lptmc.jussieu.fr).

One contribution of 18 to a Theme Issue 'Geometry of interfaces: topological complexity in biology and materials'.

Received 18 October 2011
Accepted 10 January 2012

This journal is © 2012 The Royal Society

Downloaded from rsfs.royalsocietypublishing.org on November 12, 2012

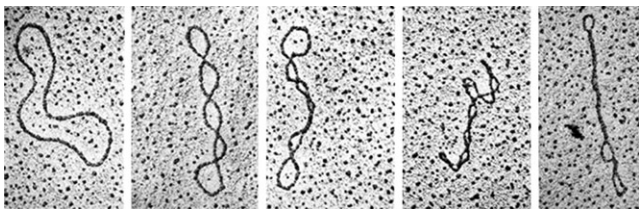

Figure 1. Supercoiling: different topological states (topoisomers) of circular DNA molecules. Reproduced with permission from Kornberg [5].

When one extremity of a ribbon is rotated around the local tangent to its axis, the ribbon modifies its conformation by splitting up the imposed rotation into two complementary contributions: its twist and its writhe.

2.1. Twist

The ribbon twist is equal to the excess of torsion induced around its own axis. If $\boldsymbol{r}(s)$ defines the ribbon axis trajectory, with s the arc-length along the DNA path, then we can define the tangent, normal and binormal vectors, respectively, by

$$\left.\begin{aligned} \boldsymbol{t}(s) = \frac{\mathrm{d}\boldsymbol{r}/\mathrm{d}s}{|\mathrm{d}\boldsymbol{r}/\mathrm{d}s|}, \quad \boldsymbol{n}(s) = \frac{\mathrm{d}\boldsymbol{t}/\mathrm{d}s}{|\mathrm{d}\boldsymbol{t}/\mathrm{d}s|}, \\ \boldsymbol{b}(s) = \boldsymbol{t} \times \boldsymbol{n}. \end{aligned}\right\} \tag{2.1}$$

The normal vector then leads to the definition of an *intrinsic* local reference frame following the ribbon axis, called the Frenet reference frame, whose normal coincides with the principal normal vector to the curve. The twist of a ribbon can then be decomposed into the sum of the twist of the Frenet frame plus the twist of the ribbon relative to the Frenet frame [8]. The twist of a straight DNA is simply given by the *excess* number of turns of the double helix with respect to its relaxed state. For a bent DNA, the calculation is more delicate. We will explicitly express this term for a special case of interest in §5.

2.2. Writhe

The writhe of a *closed* ribbon of length L depends instead on the curve followed by the ribbon axis in the three-dimensional space. It measures the coiling of the axis, and its computation is quite complicated. It is generally evaluated through a double integral according to a method based on Gauss theorem, leading to the formula

$$\mathrm{Wr} = \frac{1}{4\pi}\int_0^L \int_0^L \frac{(\boldsymbol{r}(s) - \boldsymbol{r}(s')) \cdot (\boldsymbol{t}(s) - \boldsymbol{t}(s'))}{|\boldsymbol{r}(s) - \boldsymbol{r}(s')|^3}\, \mathrm{d}s\, \mathrm{d}s'. \tag{2.2}$$

The Gauss integral can be efficiently integrated numerically. Nevertheless, an alternative method has been introduced by Fuller [7], which has the advantage of a direct geometrical interpretation and of a more straightforward generalization to open curves [11].

Consider again the unit vector tangent to the closed ribbon, $\boldsymbol{t}(s)$. The tangent vector vertex, $T(s)$, lies on the unit sphere. As s varies from 0 to L, it describes a closed curve on this sphere, called *tangent indicatrix* [9].

Fuller's first theorem states that the writhe of the curve $\boldsymbol{r}(s)$ can be calculated from the *signed* area $\mathcal{A}$ enclosed by the tangent indicatrix $T(s)$, namely $\mathrm{Wr} = \mathcal{A}/2\pi - 1 \pmod 2$. Under a few hypotheses, Fuller's second theorem [7] permits one to get rid of this congruence when one calculates the writhe *difference* between two closed curves, $\boldsymbol{r}_1(s)$ and $\boldsymbol{r}_2(s)$. The hypotheses of the theorem impose that one of the curves can be obtained from the other by a continuous deformation in space such that (i) at any point along the curve and at any moment during the transformation, the tangent vector should assume opposite direction with respect to any other intermediate state, (ii) the curve is non-self-intersecting all along the transformation, and (iii) the tangent to the curve varies continuously. Provided these conditions, it is possible to show that the difference in writhe between the two curves corresponds to the area $\mathcal{S}$ swept out by the unique shortest geodesic arc from the running point $T_1(s)$ to the running point $T_2(s)$ on the unit sphere, divided by 2π, i.e. $\mathcal{S}/2\pi$. This allows one, in particular, to calculate the writhe of a DNA chain with respect to a referring state, that could be a straight DNA, if the deformation satisfies the previous hypotheses.

2.3. Linking number

For a filament whose ends are oriented in fixed directions, if one of them is rotated around its tangent, then the sum of the twist and the writhe variations will always correspond to the number of turns applied. This property is formalized by the famous White–Fuller theorem

$$\Delta\mathrm{Lk} = \Delta\mathrm{Tw} + \Delta\mathrm{Wr}, \tag{2.3}$$

where Lk is the filament *linking number*. For a closed ribbon, or a ribbon with clamped ends, the linking number is, therefore, a topological invariant.

3. MAGNETIC TWEEZERS: WRAPPING DNA

The effect of mechanical constraints on the topology of a single DNA molecule can be nowadays experimentally explored, thanks to magnetic tweezers manipulation. This is a single-molecule technique that permits controlled application of force and torsion on a biomolecule of interest. In a typical set-up, one extremity of a single DNA molecule is attached to a glass surface, the other

Downloaded from rsfs.royalsocietypublishing.org on November 12, 2012

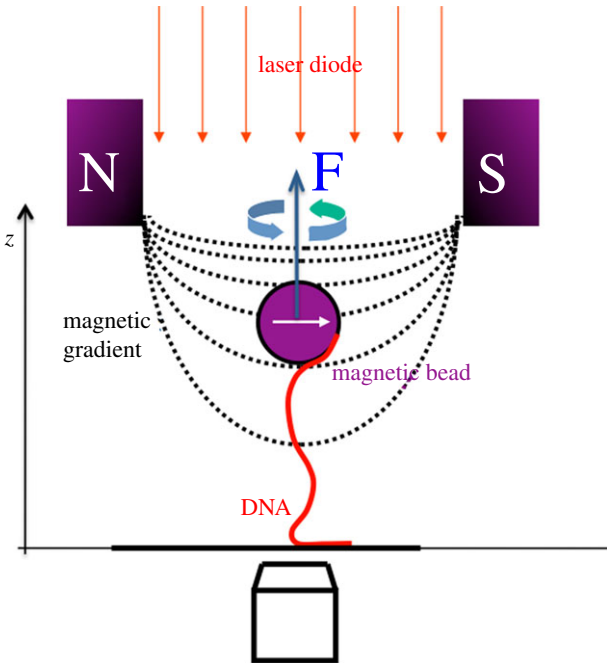

Figure 2. Schematic of the magnetic tweezers set-up. See the main text for details.

extremity to a micrometre-sized paramagnetic bead. Permanent magnets induce a magnetic moment in the magnetic bead, which experiences a force owing to the magnetic field gradient of the magnets. Moreover, the magnetic bead can be rotated to a controlled number of turns by rotating the magnets (figure 2).

The effect of torsion on a DNA molecule is not very different from what we can experience in everyday life by twisting a rope. At high pulling force, the application of a torque twists the molecule on its axis. If the pulling force is now released, while maintaining constant the bead rotation, the twist of the molecule becomes unstable and the molecule tends to writhe on itself, forming typical super-coiled structures called *plectonemes*. A plectoneme is a loop of helices twisted together as we are used to experience with electric cables.

The instability that converts twist to writhe is the result of a competition between bending and twisting energies, the latter becoming too large for large torsion. The transition to plectonemes arises at a critical torque [13], and plectoneme formation absorbs a significant portion of the mechanical stress exerted on the DNA. Since in plectonemes, the DNA wraps on itself, their formation shortens the molecule, and is therefore detectable by measuring, at constant force, the height of the magnetic bead as a function of the number of turns n applied, i.e. of the linking number variation $\Delta\mathrm{Lk} = n$. The rotation response of DNA has been studied in detail [13–18] and we now dispose of good fitting functions that may be adjusted to the rotation–extension curves very precisely.

Magnetic tweezers have also given spectacular results on the mechanics of DNA [19–21], revealing unexpected structural changes, such as the existence of over-stretched S-DNA [22] or over-twisted P-DNA [23], and allowing the study of important conformational transitions such

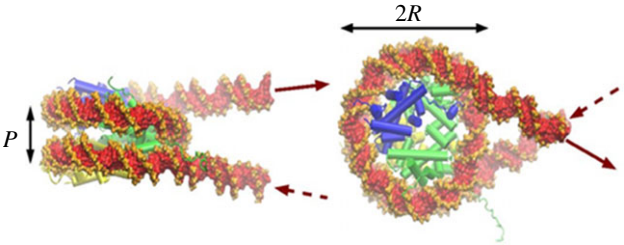

Figure 3. Structure of the nucleosome. In green, the histone tetramer $(H3\text{-}H4)_2$, in blue and yellow, the two histone dimers (H2A-H2B). The figure has been obtained starting from the crystallographic structure [31], to which were added two short entering and exiting DNA segments (courtesy of Richard Lavery).

as the formation of cruciforms [24]. While the biological relevance of cruciforms is known, the existence *in vivo* of the two unexpected altered DNA forms has still to be demonstrated. However, it seems plausible that they can appear, at least locally, owing to DNA–protein interaction. The second field where optical and magnetic tweezers have given very interesting results is precisely the study on the interaction of DNA with enzymes. These studies include the action of topoisomerases [25,26], of RNAP during transcription initiation [27,28], or of remodelling enzymes [29]. For a more exhaustive review on tweezers set-up and applications, see Lavelle *et al.* [30].

4. DNA IN THE EUKARYOTIC CELL: CHROMATIN AND CHROMATIN FIBRE

Dealing with metres of DNA in a 10 nm nucleus is, evidently, an overwhelming problem. In the nucleus of eukaryotic cells, the genetic material is organized into a complex DNA–protein assembly, called chromatin. The nucleosome (figure 3) is the fundamental unit of chromatin. It is formed by a spool of proteins (histones) on which 147 DNA base pairs (bp) are wrapped in about 1.65 turns. Nucleosomes are more or less regularly spaced on the genome, with a repeat length N_r of the order of 200 bp (but rather variable depending on organisms, tissues, genomic regions and approximately in the range 155 to 240 bp). Nucleosome core particles (NCPs) form then a bead on a string array, with short stretches of bare DNA—the linker-DNA—connecting adjacent nucleosomes.

The higher levels of organization remain largely speculative. However, it is generally accepted that attractive interactions between nucleosomes [32] fold this array into a fibre about 30 nm in diameter (figure 4).

Although fibres have been observed *in vitro*, their existence *in vivo* remains an open—and highly debated—question [33,34] since most attempts to visualize these fibres *in vivo* have failed so far, except for some rare images obtained in nuclei which are transcriptionally largely inactive (chicken erythrocytes and echinoderm sperm) [35,36].

Since the entry–exit DNA should be phased with respect to the protein core, the precise orientation of a nucleosome with respect to the previous one is largely

Downloaded from rsfs.royalsocietypublishing.org on November 12, 2012

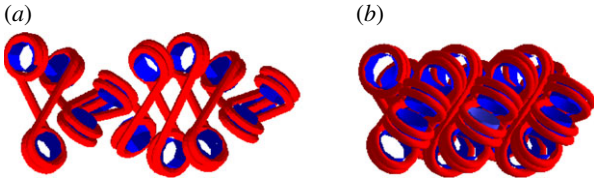

Figure 4. One of the many possible models of chromatin fibre, in a more condensed (*a*) and a less condensed (*b*) configuration. The regular spacing between nucleosomes allows for the formation of a compact structure, probably stabilized by stacking nucleosome–nucleosome interactions.

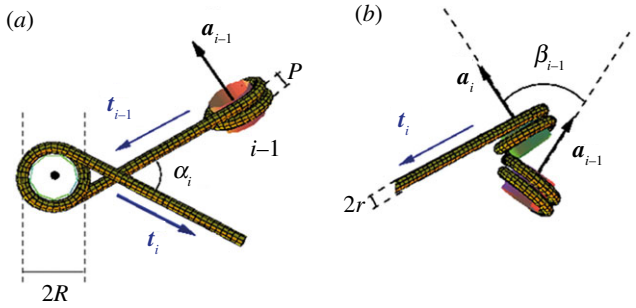

Figure 5. Schematic of the DNA winding pattern along two neighbouring nucleosomes in the two-angle model. (*a*) View down the NCP axis $\boldsymbol{a}_i$. (*b*) View down the linker direction $\boldsymbol{t}_{i-1}$. The angle α is the dihedral angle ($\boldsymbol{t}_{i-1}$, $\boldsymbol{a}_i$, $\boldsymbol{t}_i$) and β the dihedral angle ($\boldsymbol{a}_{i-1}$, $\boldsymbol{t}_{i-1}$, $\boldsymbol{a}_i$) standing for the twist (*modulo* 2π) of the DNA linker.

determined by the linker-DNA length and by the torsional constraint applied to the fibre. The shortness of the linker DNA is indeed hardly compatible with its bending, so that one can reasonably assume the linkers as straight (except, of course, in the case of additional protein binding). This assumption led Woodcock *et al.* [37] to propose a simple, geometrical model for the chromatin structure at the 30 nm scale, called the *two-angle model*, which describes the fibre by the following three parameters: the entry–exit angle α, the rotational angle β and the linker length (figure 5).

We believe that the physical properties of the chromatin fibre may govern the structural changes necessary for the functioning and dynamics of chromatin. Since the chromatin fibre is, *in vivo*, organized in loops with fixed end, the linking number is generally a conserved quantity. We therefore proposed a method to calculate the twist, writhe and linking number of the embedded DNA [38], based on the work of Fuller [6], for any conformation of the fibre obtained using the canonical two-angle model of Woodcock *et al.* [37]. The possibility to calculate these topological quantities provides an important element for modelling the dynamic behaviour of fibres. Following this idea, we proposed a possible mechanism for the condensation of chromatin during mitosis [39].

5. TOPOLOGY INTO THE FIBRE

5.1. Reference crystallographic relaxed state

The number n_{NCP} of bp in contact with the protein core, and therefore the angle α, may vary as a consequence of a partial unwrapping of the DNA. A reference value for α is obtained from the X-ray crystallographic data, giving a superhelix path with a radius $R = 4.18$ nm and pitch $P = 2.39$ nm [40]. The crystallographic superhelix corresponds thus to 1.65 turns, this covering $n^0_{\mathrm{NCP}} = 126$ bp and, consequently, the reference angle α_0 amounts to $\alpha_0 = 1.65 \times 2\pi - 3\pi = 0.3\pi$ or 0.94 rad (54°).

The angle β depends on the degree of overtwist of the linker, but also on the linker length itself and depends on α in a non-trivial way: the position of the DNA grooves at the exiting point of the previous NCP introduces indeed a phase that has to be taken into account. It is useful to introduce a reference value β_0, corresponding to the crystallographic NCP structure with *relaxed* (untwisted) linkers, which amounts to $\beta_0 = 2\pi(N_{\mathrm{r}} - n^0_{\mathrm{NCP}})/h_0$, with h_0 the number of bp per helical turn in a straight and relaxed DNA in the classical B form.

5.2. Twist in the fibre

In the two-angle model, the repeat is composed of two parts: a superhelical DNA with solenoidal shape in the NCP, followed by a straight linker DNA, eventually twisted. The left-handed solenoid described by the DNA axis is represented by the parametric curve $\boldsymbol{r}(\sigma) = (-R\cos(2\pi\sigma/P),\ R\sin(2\pi\sigma/P),\ \sigma)$, with σ the arc-length along the NCP axis, related to the arc-length along the solenoidal curve, s, by the relation $\mathrm{d}s = |\mathrm{d}\boldsymbol{r}/\mathrm{d}\sigma|\,\mathrm{d}\sigma$.

Since the twist is an extensive quantity, its calculation for DNA in a fibre can be done at the level of a single nucleosome as a function of angles α and β following the derivation of White & Bauer [8].

The overall twist per nucleosome tw can, therefore, be expressed as the sum of two twist contributions: (i) from the linker-DNA, $\mathrm{tw}_{\mathrm{linker}} = (N_{\mathrm{r}} - n_{\mathrm{NCP}})/h$ and (ii) from the NCP, $\mathrm{tw}_{\mathrm{NCP}} = n_{\mathrm{NCP}}/h' - \tau(3\pi + \alpha)/2\pi$, where we indicate with h (respectively, h') the number of bp in a linker (respectively, NCP) DNA period. The last term in $\mathrm{tw}_{\mathrm{NCP}}$ is the twist contribution owing to the *bending* of the DNA axis. The tortuosity τ corresponds to the absolute value of the total torsion T obtained by integrating the local torsion $\tau_{\mathrm{L}} = -2\pi P/(4\pi^2R^2 + P^2)$ over one helical turn of the DNA axis path in the NCP [8] and finally amounts to $\tau = P/\sqrt{4\pi^2R^2 + P^2}$.

It is now possible to introduce an explicit twist dependence on α and β, by calculating tw and β as a function of the number of wrapped bp n_{NCP}, then recombining the two expressions. Moreover, in general biological applications it is usual to refer to a *relative*

Downloaded from rsfs.royalsocietypublishing.org on November 12, 2012

DNA twist, i.e. to calculate the difference between the total twist tw and a reference twist tw_0, which corresponds to the twist of a straight and relaxed B-DNA of the same length. After subtraction of this term, the final expression obtained is

$$\Delta\mathrm{tw}(\alpha,\beta) = \frac{\beta-\beta_0}{2\pi} - \tau\,\frac{\alpha-\alpha_0}{2\pi} + \Delta\,\mathrm{tw}_{\mathrm{NCP}}\,. \qquad (5.1)$$

Here $\Delta\mathrm{tw}_{\mathrm{NCP}} = 13 - n^0_{\mathrm{NCP}}/h_0 - \tau(3\pi+\alpha_0)(2\pi)$ is the difference in twist between the wrapped DNA and a corresponding straight, relaxed DNA stretch of the same length, as measured at $\alpha=\alpha_0$.

5.3. Writhe in the fibre

The writhe is known to be non-extensive and, as shown by Starostin [11], the total writhe of a curve is given by the sum of the writhes of its parts *plus* the surface of the spherical polygon composed by the set of geodesics closing each part.

However, assuming the chromatin fibre as a regular structure composed of identical repetitive nucleosomes, it is possible to calculate its writhe from the writhe of the individual units, up to a boundary term. In the case of a chromatin fibre, the DNA indicatrix $T(s)$ can indeed be naturally divided into N parts, namely the N nucleosomes, in correspondence to $\boldsymbol{t}_i = \boldsymbol{t}(s_i)$, the direction of the (straight) linker i. Denote by T_i the vertex point on the unit sphere that corresponds to $\boldsymbol{t}_i$. The total writhe of the DNA in the fibre is then given, accordingly to Starostin [11] and Barbi *et al.* [38], by the following addition rule:

$$\mathrm{Wr} = \sum_{i=1}^{N} \mathrm{wr}_{\mathrm{NCP}}(\alpha) + \frac{\mathcal{S}_{T_0T_1\ldots T_N}}{2\pi}. \qquad (5.2)$$

Here, $\mathrm{wr}_{\mathrm{NCP}}(\alpha)$ is the writhe of the ith nucleosome *whose indicatrix had been closed by a geodesic*, while $\mathcal{S}_{T_0T_1\ldots T_N}/2\pi$ is the area enclosed in the spherical polygon of vertices $T_0, T_1, \ldots, T_N$, and represents the writhe of the 'carrying' structure formed by the sequence of linkers, or *linker skeleton*.

This second term $\mathcal{S}_{T_0T_1\ldots T_N}$ in equation (5.2) is the non-extensive contribution, given by the signed area of the spherical polygon connecting all points T_i that correspond to the linker directions. Nevertheless, it should be very useful, at this point, to 'remove' the non-extensivity by an appropriate partition of this area. Once chosen an arbitrary point C on the unit sphere, the area $\mathcal{S}_{T_0T_1\ldots T_N}$ can also be written as $\mathcal{S}_{T_0T_1\ldots T_N} = \sum_{i=1}^{N} \mathcal{S}_{CT_{i-1}T_i} + \mathcal{S}_{CT_NT_0}$. This partition allows a natural decomposition of the writhe into single nucleosome contributions: up to a single boundary term $\mathcal{S}_{CT_NT_0}/2\pi$, the writhe can be expressed as the sum $\mathrm{Wr} = \sum_{i=1}^{N} \mathrm{wr}_i|_C$, where we define the writhe $\mathrm{wr}_i|_C$ of nucleosome i *with respect to point* C as

$$\mathrm{wr}_i|_C = \mathrm{wr}_{\mathrm{NCP}}(\alpha) + \frac{\mathcal{S}_{CT_{i-1}T_i}}{2\pi}. \qquad (5.3)$$

Moreover, there exists a special point, $C=F$, defined by the director of the *fibre axis*, for which $\mathcal{S}_{FT_{i-1}T_i} = \mathcal{S}(\alpha,\beta)$ is the same for all the nucleosomes (figure 6). For this particular choice, we can define an effective

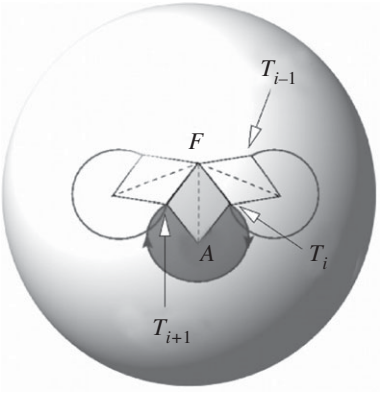

Figure 6. A schematic of the writhe calculation for a nucleosome in a regular fibre. Scales and length have been arbitrarily chosen for the sake of clarity. The curve represents the tangent indicatrix of DNA in the fibre. Point T_i represents the vertex of the ith linker tangent vector. The circular part corresponds to the indicatrix of the DNA wrapping around the nucleosome. The central point is the direction of the fibre axis. The surface $\mathcal{S}(\alpha,\beta)$ of equation (5.4) corresponds to the spherical triangle FT_iT_{i+1}.

writhe per nucleosome, $\mathrm{wr}(\alpha,\beta)$, such that

$$\mathrm{wr}_i|_F = \mathrm{wr}(\alpha,\beta) = \mathrm{wr}_{\mathrm{NCP}}(\alpha) + \frac{\mathcal{S}(\alpha,\beta)}{2\pi}. \qquad (5.4)$$

5.4. Linking number per nucleosome

The particular choice of the reference point F leads to an expression for the writhe which is not only additive, but also provides identical contributions for each nucleosome, thus supplying for a consistent definition of a writhe *per nucleosome* $\mathrm{wr}(\alpha,\beta)$, independent of the fibre length N. Summing up the twist and writhe contributions, we have finally the following expression for the DNA linking number excess in the fibre $\Delta\mathrm{Lk}$:

$$\frac{\Delta\mathrm{Lk}}{N} = \mathrm{wr}(\alpha,\beta) + \frac{\beta-\beta_0(\alpha)}{2\pi} - \tau\,\frac{\alpha-\alpha_0}{2\pi} + \Delta\,\mathrm{tw}_{\mathrm{NCP}}. \qquad (5.5)$$

5.5. Possible extensions to irregular fibres

Up to now, we have considered perfectly regular fibres. In this case, the fibre is always straight, its writhe is zero, and the DNA linking number calculated here can be associated with the fibre twist: a change in α and β will indeed modify the fibre architecture and consequently induce a rotation of one fibre end with respect to the other.

However, it has been pointed out that consecutive nucleosomes may have significantly altered topology owing to alternative nucleosome spacing [41] and topological models accounting for alternating linker DNA crossings [42] as well as for irregular spacing between nucleosomes [43] have been proposed. In principle, alternate nucleosomal spacing or alternate linker DNA crossing[1] can be accounted for by our model, through a redefinition of the repetition unit in the fibre:

[1]A linker DNA bending can be included in the model by adding one more local angle [44].

Downloaded from rsfs.royalsocietypublishing.org on November 12, 2012

this would imply a decomposition of the fibre into di-nucleosomes, the calculation of the linking number contribution per di-nucleosome with respect to the local fibre axis, and a redefinition of the fibre backbone based on the new partition. The calculation of the di-nucleosome linking number may be quite cumbersome but it can be obtained, and the principle of calculation remains the same.

On the other hand, linker DNA folding heterogeneity can be also addressed. An extension of the previous calculation can be made to include fibres for which the structural parameters α and β change from nucleosome to nucleosome in a periodic way along the fibre. In that case, some additional terms should be included in the DNA linking number expression, essentially owing to the different orientation of the *local* fibre axis with respect to a reference straight axis. Such additional terms can therefore be associated with the bending of the fibre axis, i.e. with the fibre writhe, and the total DNA linking number can therefore be rewritten as the sum of *fibre twist* and *writhe* [38].

6. WRAPPING CHROMATIN FIBRES

Micromanipulation by magnetic tweezers of chromatin fibres has been realized by the team of Jean-Louis Viovy [44–46]. Chromatin fibres of tens of nucleosomes, reconstituted *in vitro* and inserted between two fragments of naked DNA are manipulated—stretched and twisted.

The rotation–extension response of the nucleosome assembly showed rather unexpected results. Unlike what was observed for DNA, the fibres can absorb a very high number of turns, with little or no change in length (high torsional resilience). Intuitively, these results imply that nucleosomes must be able to store a portion of the torsion induced in the fibre. Calculating the topological parameters of the fibre is an essential step in order to interpret these results. We have therefore proposed a statistical physics model, including the existence of structural transitions of the nucleosome between three different states, characterized by different topological contributions to the fibre linking number [45]. These three states, previously identified in minicircles studies [47,48], are indeed characterized by a different pathway for the entering and exiting linker DNAs: the *negatively crossed* state corresponds to the standard crystallographic structure; in the *positively crossed* state, the two linker DNAs cross instead in the opposite, positive way; and in the *open* state, DNA is partially unwrapped from the NCP and linker DNAs do not cross any more (figure 7). The corresponding Lk contributions *per nucleosome* can be calculated as previously described and give, respectively, $\mathrm{Lk}_{\mathrm{neg}} = -1.4$, $\mathrm{Lk}_{\mathrm{open}} = -0.7$, $\mathrm{Lk}_{\mathrm{pos}} = -0.4$. The free energies for the three conformations can be estimated experimentally. The stability of the different states eventually depends on the applied torque: the application of a positive (respectively, negative) torque to the fibre will favour the states with the most positive (respectively, negative) linking number *per nucleosome*. The resulting dynamic equilibrium between the different conformations acts, therefore, as a topological buffer, absorbing the additional torsion, thanks to the rearrangement of the internal nucleosome structure [45].

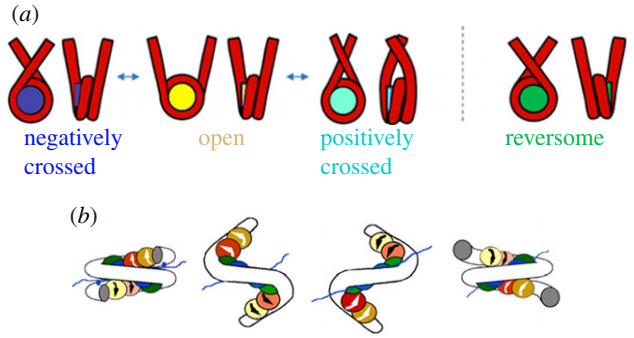

Figure 7. (*a*) The four states of the nucleosome discussed in the main text. (*b*) An image of the chiral transition of the nucleosome from the standard (crystallographic) conformation into the reversome state. Here, histones are represented by the coloured spheres and DNA by the white tube.

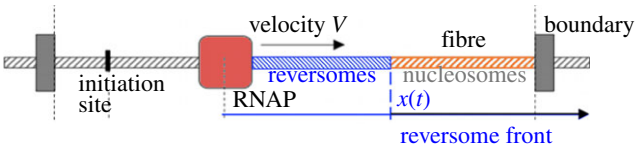

Figure 8. Schematic of the progress of a reversome front (blue) along a compact fibre of nucleosomes, induced by the advancing RNAP (red square). The two ends of the fibre are supposed to be clamped in a loop, as frequently observed in cells.

7. A NEW NUCLEOSOME STATE: THE REVERSOME

Even more unexpected, chromatin fibres display a strong hysteretic behaviour when submitted to extensive positive torsion [46]. Again, this effect can be explained by a structural rearrangement of individual nucleosomes, but implying this time a much larger deformation, with a Lk variation of about two turns per nucleosome. The altered form should be metastable in order to explain the presence of hysteresis, and has to be stabilized by the application of a large positive torque. If magnetic tweezers measurements allowed one to deduce the value of Lk for this altered form of the nucleosome, its precise structure was completely unknown. Relying on the analysis of the nucleosome normal modes to identify its flexible parts, we have obtained a coarse-grained model of the nucleosome, that we have studied by means of Brownian dynamics simulations. In the simulations, an inversion of chirality of the nucleosome is induced by the application of an external torque (and provided that linker DNAs are in the open configuration) [46,49]. The resulting structure is a right-handed nucleosome, that we named *reversome*, for *rever*sed nucleo*some* (figure 7). Calculations of the linking number contribution for this mirror-inversed nucleosome (with a slightly different α) give $\mathrm{Lk}_{\mathrm{rev}} \simeq 0.85$, in agreement with the experimental estimation of a linking number difference of about two turns. More recently, we used the same experimental

Downloaded from rsfs.royalsocietypublishing.org on November 12, 2012

Figure 9. Analogy between (*a*) the reversome transition and (*b*) the local inversion of spires in a telephone cord. The nucleosome to reversome transition is obtained by means of Brownian dynamics simulations on a coarse-grained model [55].

and theoretical methods to study fibres with and without an additional protein known to compact the fibre, the linker histone H5, and showed that linker histone incorporation maintains chromatin fibre plasticity [44].

8. PERSPECTIVES: THE 'REVERSOME WAVE'

Single fibre micromanipulation experiments suggest the existence of an inverted structure of the nucleosome, the reversome, stabilized by a significantly high torsional stress. This plasticity may play a role *in vivo*, if a torque constrains the fibre. As we have discussed, this is indeed the case in the elongation phase of transcription, when DNA screws through the RNAP, turning on its axis. We then wanted to address the broader question of whether and how transcription may take place in a condensed fibre, characterized by a regular array of nucleosomes stacked on each other (see again figure 4). In these conditions, steric hindrance prevents nucleosomes to move and change conformation. However, the first nucleosome, at the border between the condensed fibre and its decondensed part where transcription is in progress, is free to move. It will therefore pass to its reversome state under the effect of the high torque exerted by the incoming polymerase. After the transition, the torque on the fibre is partially relaxed, since about two turns are absorbed in the transition. However, it starts to increase again with the progression of the RNAP and eventually reaches the critical torque required to induce a new transition. The following nucleosome then passes to the reversome state and so on, with a *domino* effect, that forms a 'reversome front' progressing along the fibre (figure 8). This mechanism acts as a 'topological buffer' to absorb excess of positive supercoiling [50]. We have estimated the speed of this reversome front, which results to be about 10 times larger than the speed of the RNAP, thus indicating that it spreads rapidly far from the transcribing region. This model mainly applies to intense transcription events, where local loss of histones during passage of the polymerase is observed [3,51]. In that case, in the vicinity of the polymerase, elongation factors [3,52] help to destabilize nucleosomes (and reversomes, which are less stable), while complete reversome transition could happen farther downstream.

Although this scenario remains for the moment only a speculative suggestion, recent experimental results [53] showed a wave of destabilization of nucleosomes, which grows very rapidly along the fibre, about 10 times faster than the motion of the RNAP. These observations can be interpreted in the frame of our model [54], and possibly lead to a first verification of our hypothesis.

In conclusion, if DNA behaves as an electric cable, the nucleosome to reversome transition makes the chromatin fibre similar to a telephone cord (figure 9). An increasing linking number can not only be stored in the cord twist and writhe, but also in a third form of distortion: some of the telephone cord spires can be inverted, thus modifying locally the *internal* architecture of the cord, and relaxing the torsional stress elsewhere. Dealing with topological features of DNA represents an essential and a rich tool in order to understand and model biological processes, either *in vitro* or *in vivo*, helping in deciphering the underlying physical and mechanical constraints that can suggest new scenarios for complex phenomena.

REFERENCES

1 Cook, P. R. 1999 The organization of replication and transcription. *Science* **284**, 1790–1795. (doi:10.1126/science.284.5421.1790)
2 Liu, L. F. & Wang, J. C. 1987 Supercoiling of the DNA template during transcription. *Proc. Natl Acad. Sci. USA* **84**, 7024–7027. (doi:10.1073/pnas.84.20.7024)
3 Lavelle, C. 2007 Transcription elongation through a chromatin template. *Biochimie* **89**, 516–527. (doi:10.1016/j.biochi.2006.09.019)
4 Vinograd, J., Lebowitz, J., Radloff, R., Watson, R. & Laipis, P. 1965 The twisted circular form of polyoma viral DNA. *Proc. Natl Acad. Sci. USA* **53**, 1104–1111. (doi:10.1073/pnas.53.5.1104)
5 Kornberg, A. 1980 *DNA replication*, p. 29. San Francisco, CA: W. H. Freeman.
6 Fuller, F. B. 1971 The writhing number of a space curve. *Proc. Natl Acad. Sci. USA* **68**, 815–819. (doi:10.1073/pnas.68.4.815)
7 Fuller, F. B. 1978 Decomposition of the linking number of a closed ribbon, a problem from molecular biology. *Proc.*

Downloaded from rsfs.royalsocietypublishing.org on November 12, 2012

Natl Acad. Sci. USA **75**, 3557–3561. (doi:10.1073/pnas.75.8.3557)
8 White, J. H. & Bauer, W. R. 1982 Calculation of the twist and writhe for representative models of DNA. *J. Mol. Biol.* **189**, 329–341. (doi:10.1016/0022-2836(86)90513-9)
9 Maggs, A. C. 2001 Writhing geometry at finite temperature: random walks and geometric phases for stiff polymers. *J. Chem. Phys.* **114**, 5888–5896. (doi:10.1063/1.1353545)
10 Rossetto, V. & Maggs, A. C. 2003 Writhing geometry of open DNA. *J. Chem. Phys.* **21**, 9864–9874. (doi:10.1063/1.1569905)
11 Starostin, E. L. 2005 On the writhe of non-closed curves. In *Physical and numerical models in knot theory including applications to the life sciences*, vol. 36 (eds J. Calvo, K. Millett & E. Rawdon & A. Stasiak), pp. 525–545. Singapore: World Scientific. (doi:10.1142/97898127 03460_0026)
12 van der Heijden, G. H. M., Peletier, M. A. & Planque, R. 2007 On end rotation for open rods undergoing large deformations. *Q. Appl. Math.* **65**, 385–402.
13 Moroz, J. D. & Nelson, P. 1997 Torsional directed walks, entropic elasticity, and DNA twist stiffness. *Proc. Natl Acad. Sci. USA* **94**, 14 418–14 422. (doi:10.1073/pnas.94.26.14418)
14 Marko, J. F. & Siggia, E. D. 1995 Statistical mechanics of supercoiled DNA. *Phys. Rev. E* **52**, 2912–2938. (doi:10.1103/PhysRevE.52.2912)
15 Bouchiat, C. & Mezard, M. 1998 Elasticity theory of a supercoiled DNA molecule. *Phys. Rev. Lett.* **80**, 1556–1559. (doi:10.1103/PhysRevLett.80.1556)
16 Neukirch, S., van der Heijden, G. H. M. & Thompson, J. M. T. 2002 Writhing instabilities of twisted rods: from infinite to finite length. *J. Mech. Phys. Solids* **50**, 1175–1191. (doi:10.1016/S0022-5096(01)00130-2)
17 Neukirch, S. 2004 Extracting DNA twist rigidity from experimental supercoiling data. *Phys. Rev. Lett.* **93**, 198107. (doi:10.1103/PhysRevLett.93.198107)
18 Clauvelin, N., Audoly, B. & Neukirch, S. 2009 Elasticity and electrostatics of plectonemic DNA. *Biophys. J.* **96**, 3716–3723. (doi:10.1016/j.bpj.2009.02.032)
19 Smith, S., Finzi, L. & Bustamante, C. 1992 Direct mechanical measurements of the elasticity of single DNA molecules by using magnetic beads. *Science* **258**, 1122–1126. (doi:10.1126/science.1439819)
20 Bustamante, C., Marko, J. F., Siggia, E. D. & Smith, S. 1994 Entropic elasticity of lambda-phage DNA. *Science* **265**, 1599–1600. (doi:10.1126/science.8079175)
21 Strick, T. R., Allemand, J.-F., Bensimon, D., Bensimon, A. & Croquette, V. 1996 The elasticity of a single supercoiled DNA molecule. *Science* **271**, 1835–1837. (doi:10.1126/science.271.5257.1835)
22 Cluzel, P., Lebrun, A., Heller, C., Lavery, R., Viovy, J.-L., Chatenay, D. & Caron, F. 1996 DNA: an extensible molecule. *Science* **271**, 792–794. (doi:10.1126/science.271.5250.792)
23 Allemand, J. F., Bensimon, D., Lavery, R. & Croquette, V. 1998 Stretched and overwound DNA forms a Pauling-like structure with exposed bases. *Proc. Natl Acad. Sci. USA* **95**, 14 152–14 157. (doi:10.1073/pnas.95.24.14152)
24 Ramreddy, T., Sachidanandam, R. & Strick, T. R. 2011 Real-time detection of cruciform extrusion by single-molecule DNA nanomanipulation. *Nucleic Acids Res.* **39**, 4275–4283. (doi:10.1093/nar/gkr008)
25 Dekker, N. H., Rybenkov, V. V., Duguet, M., Crisona, N. J., Cozzarelli, N. R., Bensimon, D. & Croquette, V. 2002 The mechanism of type IA topoisomerases. *Proc. Natl Acad. Sci. USA* **99**, 12 126–12 131. (doi:10.1073/pnas.132378799)
26 Charvin, G., Bensimon, D. & Croquette, V. 2003 Single-molecule study of DNA unlinking by eukaryotic and prokaryotic type-II topoisomerases. *Proc. Natl Acad. Sci. USA* **100**, 9820–9825. (doi:10.1073/pnas.1631550100)
27 Revyakin, A., Ebright, R. H. & Strick, T. R. 2004 Promoter unwinding and promoter clearance by RNA polymerase: detection by single-molecule DNA nanomanipulation. *Proc. Natl Acad. Sci. USA* **101**, 4776–4780. (doi:10.1073/pnas.0307241101)
28 Revyakin, A., Liu, R. C., Ebright, H. & Strick, T. R. 2006 Abortive initiation and productive initiation by RNA polymerase involve DNA scrunching. *Science* **314**, 1139–1143. (doi:10.1126/science.1131398)
29 Lavelle, C., Praly, E., Bensimon, D., Le Cam, E. & Croquette, V. 2011 Nucleosome remodelling machines and other molecular motors observed at the single molecule level. *FEBS J.* **278**, 3596–3607. (doi:10.1111/j.1742-4658.2011.08280.x)
30 Lavelle, C., Victor, J.-M. & Zlatanova, J. 2010 Chromatin fiber dynamics under tension and torsion. *Int. J. Mol. Sci.* **11**, 1557–1579. (doi:10.3390/ijms11041557)
31 Davey, C. A., Sargent, D. F., Luger, K., Maeder, A. W. & Richmond, T. J. 2002 Solvent mediated interactions in the structure of the nucleosome core particle at 1.9 Å resolution. *J. Mol. Biol.* **319**, 1097–1113. (doi:10.1016/S0022-2836(02)00386-8)
32 Scheffer, M. P., Eltsov, M., Bednar, J. & Frangakis, A. S. In press. Nucleosomes stacked with aligned dyad axes are found in native compact chromatin in vitro. *J. Struct. Biol.* (doi:10.1016/j.jsb.2011.11.020)
33 Maeshima, K., Hihara, S. & Eltsov, M. 2010 Chromatin structure: does the 30-nm fibre exist *in vivo*? *Curr. Opin. Cell Biol.* **22**, 291–297. (doi:10.1016/j.ceb.2010.03.001)
34 Fussner, E., Ching, R. W. & Bazett-Jones, D. P. 2011 Living without 30 nm chromatin fibers. *Trends Biochem. Sci.* **36**, 1–6. (doi:10.1016/j.tibs.2010.09.002)
35 Scheffer, M. P., Eltsov, M. & Frangakis, A. S. 2011 Evidence for short-range helical order in the 30-nm chromatin fibers of erythrocyte nuclei. *Proc. Natl Acad. Sci. USA* **108**, 16 992–16 997. (doi:10.1073/pnas.1108268108)
36 Horowitz, R. A., Agard, D. A., Sedat, J. W. & Woodcock, C. L. 1994 The three-dimensional architecture of chromatin *in situ*: electron tomography reveals fibers composed of a continuously variable zig-zag nucleosomal ribbon. *J. Cell Biol.* **125**, 1–10. (doi:10.1083/jcb.125.1.1)
37 Woodcock, C. L., Grigoryev, S. A., Horowitz, R. A. & Whitaker, N. A. 1993 Chromatin folding model that incorporates linker variability generates fibers resembling the native structures. *Proc. Natl Acad. Sci. USA* **90**, 9021–9025. (doi:10.1073/pnas.90.19.9021)
38 Barbi, M., Mozziconacci, J. & Victor, J. M. 2005 How the chromatin fiber deals with topological constraints. *Phys. Rev. E* **71**, 031 910. (doi:10.1103/PhysRevE.71.031910)
39 Mozziconacci, J., Lavelle, C., Barbi, M., Lesne, A. & Victor, J. M. 2006 A physical model for the condensation and decondensation of eukaryotic chromosomes. *FEBS Lett.* **580**, 368–372. (doi:10.1016/j.febslet.2005.12.053)
40 Luger, K., Maeder, A. W., Richmond, R. K., Sargent, D. F. & Richmond, T. J. 1997 Crystal structure of the nucleosome core particle at 2.8 Å resolution. *Nature* **389**, 251–259. (doi:10.1038/38444)
41 Stein, A. 1980 DNA wrapping in nucleosomes. The linking number problem re-examined. *Nucleic Acids Res.* **8**, 4803–4820. (doi:10.1093/nar/8.20.4803)
42 Worcel, A., Strogatz, S. & Riley, D. 1981 Structure of chromatin and the linking number of DNA. *Proc. Natl Acad. Sci. USA* **78**, 1461–1465. (doi:10.1073/pnas.78.3.1461)

Downloaded from rsfs.royalsocietypublishing.org on November 12, 2012

43 Grigoriev, S. A. & Ioffe, L. B. 1981 The dependence of the linking number of a circular minichromosome upon the shape and the orientation of its nucleosomes. *FEBS Lett.* **130**, 43–46. (doi:10.1016/0014-5793(81)80661-8)

44 Recouvreux, P., Lavelle, C., Barbi, M., Conde e Silva, N., Le Cam, E., Victor, J.-M. & Viovy, J.-L. 2011 Linker histones incorporation mantains chromatin fiber plasticity. *Biophys. J.* **100**, 2726–2735. (doi:10.1016/j.bpj.2011.03.064)

45 Bancaud, A. *et al.* 2006 Structural plasticity of single chromatin fibers revealed by torsional manipulation. *Nat. Struct. Mol. Biol.* **13**, 444–450. (doi:10.1038/nsmb1087)

46 Bancaud, A. *et al.* 2007 Nucleosome chiral transition under positive torsional stress in single chromatin fibers. *Mol. Cell* **27**, 135–147. (doi:10.1016/j.molcel.2007.05.037)

47 De Lucia, F., Alilat, M., Sivolob, A. & Prunell, A. 1999 Nucleosome dynamics. III. histone tail-dependent fluctuation of nucleosomes between open and closed DNA conformations. Implications for chromatin dynamics and the linking number paradox. *J. Mol. Biol.* **285**, 1101–1119. (doi:10.1006/jmbi.1998.2382)

48 Sivolob, A., Lavelle, C. & Prunell, A. 2003 Sequence-dependent nucleosome structural and dynamic polymorphism. Potential involvement of histone H2B N-terminal tail proximal domain. *J. Mol. Biol.* **326**, 49–63. (doi:10.1016/S0022-2836(02)01372-4)

49 Lavelle, C., Recouvreux, P., Wong, H., Bancaud, A., Viovy, J.-L., Prunell, A. & Victor, J.-M. 2009 Right-handed nucleosome: myth or reality? *Cell* **139**, 1216–1217. (doi:10.1016/j.cell.2009.12.014)

50 Bécavin, C., Barbi, M., Victor, J.-M. & Lesne, A. 2010 Transcription within condensed chromatin: steric hindrance facilitates elongation. *Biophys. J.* **98**, 824–833. (doi:10.1016/j.bpj.2009.10.054)

51 Kulaeva, O. I. & Studitsky, V. M. 2010 Mechanism of histone survival during transcription by RNA polymerase II. *Transcription* **1**, 85–88. (doi:10.4161/trns.1.2.12519)

52 Workman, J. L. 2006 Nucleosome displacement in transcription. *Genes Dev.* **20**, 2009–2017. (doi:10.1101/gad.1435706)

53 Petesch, S. J. & Lis, J. T. 2008 Rapid, transcription-independent loss of nucleosomes over a large chromatin domain at Hsp70 loci. *Cell* **134**, 74–84. (doi:10.1016/j.cell.2008.05.029)

54 Zlatanova, J. & Victor, J. M. 2009 How are nucleosomes disrupted during transcription elongation? *HFSP J.* **3**, 373–378. (doi:10.2976/1.3249971)

55 Lavelle, C., Bancaud, A., Recouvreux, P., Barbi, M., Victor, J.-M. & Viovy, J.-L. 2011 Chromatin topological transitions. *Prog. Theor. Phys. Suppl.* **191**, 30–39.